

# The effect of concentration ratio and type of functional group on synthesis of CNT–ZnO hybrid nanomaterial by an in situ sol–gel process

Sekineh Hosseini Largani<sup>1</sup> · Mohammad Akbarzadeh Pasha<sup>1,2</sup>

Received: 16 November 2016 / Accepted: 11 December 2016 / Published online: 23 December 2016  
© The Author(s) 2016. This article is published with open access at Springerlink.com

**Abstract** In this research, MWCNT–ZnO hybrid nanomaterials were synthesized by a simple sol–gel process using  $\text{Zn}(\text{CH}_3\text{COO})_2 \cdot 2\text{H}_2\text{O}$  and functionalized MWCNT with carboxyl(COOH) and hydroxyl(OH) groups. Three different mass ratios of MWCNT:ZnO = 3:1, 1:1 and 1:3 were examined. The prepared nanomaterials were characterized by field emission scanning electron microscopy (FESEM), transmission electron microscopy (TEM), X-ray diffraction (XRD), energy dispersive X-ray spectroscopy (EDX) and Fourier transform infrared spectroscopy (FTIR). Successful growth of MWCNT–ZnO hybrids for both COOH and OH functional groups and all the three mass ratios were obtained. The ZnO nanoparticles attached on the surfaces of CNTs have rather spherical shapes and hexagonal crystal structure. By increasing the concentration of ZnO, the number and average size of ZnO nanoparticles decorated the body of CNTs in hybrid structures increase. By increasing the ZnO precursor, the distribution of ZnO nanoparticles that appeared on the surface of CNTs becomes more uniform. The SEM observation beside EDX analysis revealed that at the same concentration ratio the amount of ZnO loading on the surface of MWCNT-COOH is more than MWCNT-OH. Moreover, the average size of ZnO nanoparticles attached on the surface of COOH functionalized CNTs is relatively smaller than that of OH functionalized ones.

**Keywords** Carbon nanotubes · ZnO nanoparticles · CNT–ZnO hybrid · Sol–gel · Concentration ratio · Functional group

## Introduction

Because of their unique physical and chemical properties, carbon nanotubes (CNTs) are considered to be excellent candidates for many potential applications such as nanocomposite materials, nanoelectronics, catalysis and sensors [1–10]. Due to their great hardness and toughness, multiwall CNTs (MWCNTs) keep their morphology and structure even at high nanoparticle loadings [11]. It has been indicated that the CNTs' properties can be dramatically influenced by the surface modification with organic, inorganic and biological species [12–14]. Many metal oxides and sulfides such as  $\text{TiO}_2$ ,  $\text{Cu}_2\text{O}$ ,  $\text{Al}_2\text{O}_3$ ,  $\text{Co}_3\text{O}_4$ ,  $\text{MgO}$ ,  $\text{Fe}_x\text{O}_y$ ,  $\text{ZnS}$  and  $\text{CdS}$  have been used to modify the CNTs [12–15]. Zinc oxide is a semiconductor material with an energy gap of 3.37 eV and a large exciton binding energy (60 meV) at room temperature [16–19]. ZnO has remarkable physical and chemical properties including nontoxic nature, low cost, high optical activity and stability, high sensitivity of UV–Vis light and high thermal and mechanical stability at room temperature [12, 13, 16, 17, 20, 21]. These properties revealed that the ZnO is a useful material in electronics, optics, photonics, room temperature UV lasers, light emitting diodes and sensors [10–13, 20, 22]. Also it is applicable in photocatalytic degradation of organic pollutants under UV–Vis light [9, 20, 23].

MWCNT–ZnO hybrids have unique properties different from alone CNT and ZnO [9, 12]. CNTs are good electron acceptors and ZnO is a good electron donor under UV illumination. MWCNTs act as photogenerated electron acceptors to promote interfacial electron transfer process from the

✉ Mohammad Akbarzadeh Pasha  
m.akbarzadeh@umz.ac.ir

<sup>1</sup> Department of Solid State Physics, Faculty of Basic Science, University of Mazandaran, 47416-95447 Babolsar, Iran

<sup>2</sup> Research Laboratory of Carbon-based Nanostructures, Faculty of Basic Science, University of Mazandaran, Babolsar, Iran

attached ZnO to CNTs. Thus, the recombination of photo induced electron and hole would be retarded. This process enhances the photocatalytic activity of CNT–ZnO hybrid nanostructures [11]. Chen et al. synthesized ZnO nanoparticles decorated MWCNTs nanocomposite by a sol–gel method and observed that by increasing the calcination temperature from 450 to 700 °C the sizes of ZnO nanoparticles increase and the layer of coated ZnO becomes discontinuous [13]. Wang et al. conducted a report on covalent attachment of ZnO nanostructures to MWCNTs through C–N bonds. Two different morphologies of nanohybrids; flower-like ZnO on the tips of MWCNTs and ZnO nanoparticles on the surface of MWCNTs were obtained via adjusting the reaction time [12]. Yang et al. utilized an ex situ chemical preparation of CNT–ZnO nanohybrids and observed that addition of a cationic surfactant (cetyltrimethylammonium bromide; CTAB) prevents the agglomeration of ZnO nanoparticles and results in uniform distribution of ZnO nanoparticles decorated on CNTs' surfaces [10]. Our present work aims to grow the valuable CNT–ZnO nanostructures by a simple sol–gel method. Furthermore the effect of precursor concentration ratio and type of CNTs' functional group on synthesis of this nanostructure was investigated. Although CNT–ZnO nanohybrids were successfully synthesized by various methods, further exploration is still motivated [10–13, 15 and references there in]. The structure and morphology of CNT–ZnO hybrids are very sensitive to experimental parameters especially by sol–gel process [10–13, 15 and references there in, 24]. Based on our literature review the effect of functional group of CNTs on CNT–ZnO hybrid formation was not or less investigated. In this study, we report the appearance of almost perfectly spherical ZnO nanoparticles attached to the surfaces of CNTs in restricted positions which was less observed. Dependence of the size, abundance, and distribution of ZnO particles on CNT:ZnO mass ratio was clearly evidenced.

## Materials and method

In order to synthesize MWCNT–ZnO hybrid, a simple sol–gel process was applied which is similar to the route explained in Zhu et al. report [11]. Figure 1 shows the chart of the process. MWCNT with COOH and OH functional groups (denoted by MWCNT-COOH and MWCNT-OH supplied by US nano) zinc acetate [ $\text{Zn}(\text{CH}_3\text{COO})_2 \cdot 2\text{H}_2\text{O}$  supplied by Merck], diethylene glycol (DEG,  $\text{C}_4\text{H}_{10}\text{O}_3$  supplied by Merck), absolute ethanol (Merck) and deionized water were used as reactants. First, 0.33 g of  $\text{Zn}(\text{CH}_3\text{COO})_2 \cdot 2\text{H}_2\text{O}$  was dissolved in 75 ml DEG and then 3 ml deionized water was added to the solution. The solution was stirred at 160–180 °C for 5 min and kept at room temperature for 2 h to obtain ZnO sol. Subsequently, certain amount of functional MWCNTs was added to the ZnO sol and sonicated for 30 min (the mass of MWCNTs were

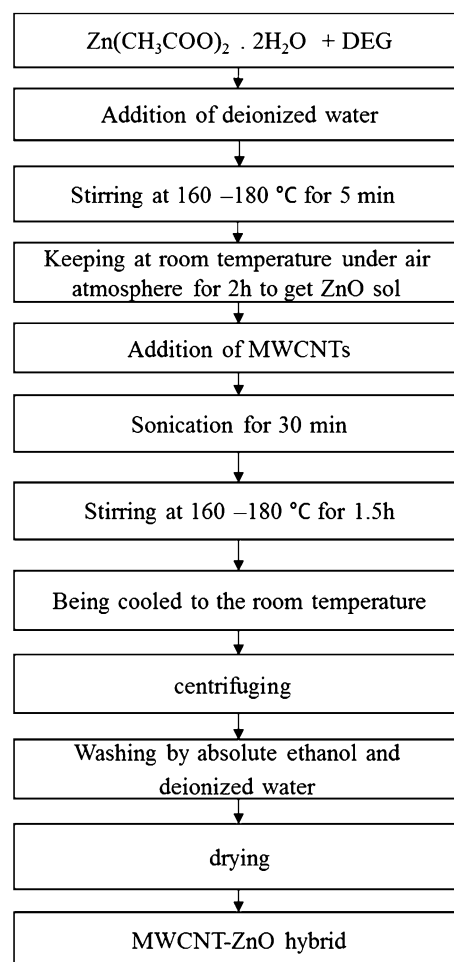


**Fig. 1** Schematic diagram of sol–gel process used to synthesize CNT–ZnO hybrids

0.36, 0.12 and 0.04 to obtain the mass ratio of MWCNTs:ZnO = 3:1, 1:1, 1:3, respectively). After that the solution was stirred at 160–180 °C for 1.5 h and then cooled down to the room temperature. Finally, the solution was centrifuged and washed with dionized water and absolute ethanol and dried in an oven at temperature of 60 °C for 48 h.

The obtained powder (MWCNT–ZnO hybrid) was characterized by field emission scanning electron microscopy (FESEM, Mira 3-XMU), X-ray diffraction (XRD, PW17C PHILIPS), energy dispersive X-ray spectroscopy (EDX analyzer attached to FESEM apparatus) and Fourier transform infrared spectroscopy (FTIR, BRUKER).

## Results and discussion

### X-ray diffraction (XRD)

In order to determine the phase and structure of the synthesized nanohybrids XRD analysis was performed.

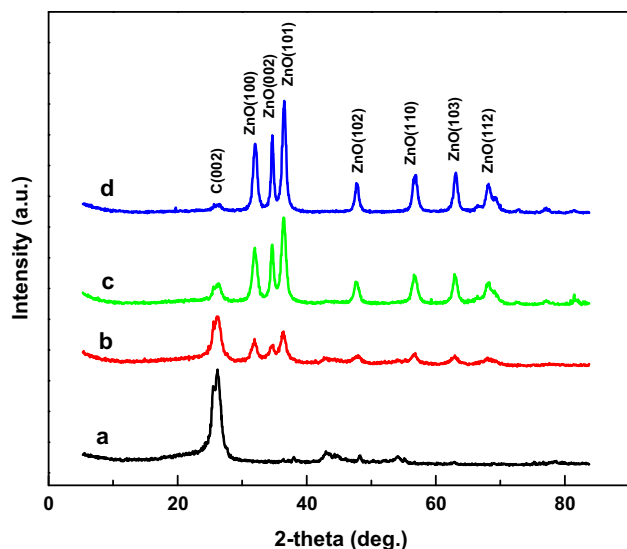


**Fig. 2** XRD patterns of the **a** MWCNT-COOH and hybrid samples, **b** MWCNT-COOH-ZnO [3:1], **c** MWCNT-COOH-ZnO [1:1] and **d** MWCNT-COOH-ZnO [1:3]

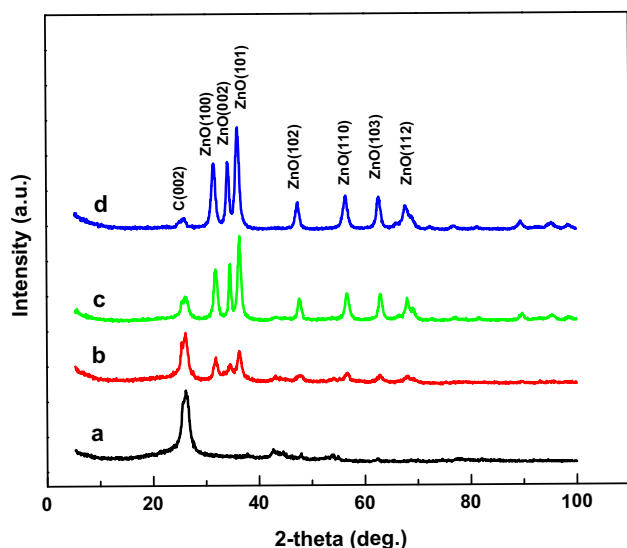


**Fig. 3** XRD patterns of the **a** MWCNT-OH and hybrid samples, **b** MWCNT-OH-ZnO [3:1], **c** MWCNT-OH-ZnO [1:1], **d** MWCNT-OH-ZnO [1:3]

Figure 2 shows XRD patterns of the raw MWCNT-COOH and MWCNT-COOH-ZnO hybrid samples. The diffraction peaks at  $2\theta = 31.7^\circ$ ,  $34.4^\circ$ ,  $36.2^\circ$ ,  $47.5^\circ$ ,  $56.5^\circ$ ,  $62.8^\circ$  and  $67.9^\circ$  can be attributed to the (100), (002), (101), (102), (110), (103) and (112) crystal plates of ZnO with hexagonal structure, respectively [9, 11, 20]. The appearance of these peaks confirms that ZnO crystallites are formed in hybrid samples. The peaks at  $2\theta = 26^\circ$  and  $44^\circ$  are attributed to the graphite structure of MWCNTs [9, 11, 20]. Between zinc oxide's peaks, the three most intense peaks

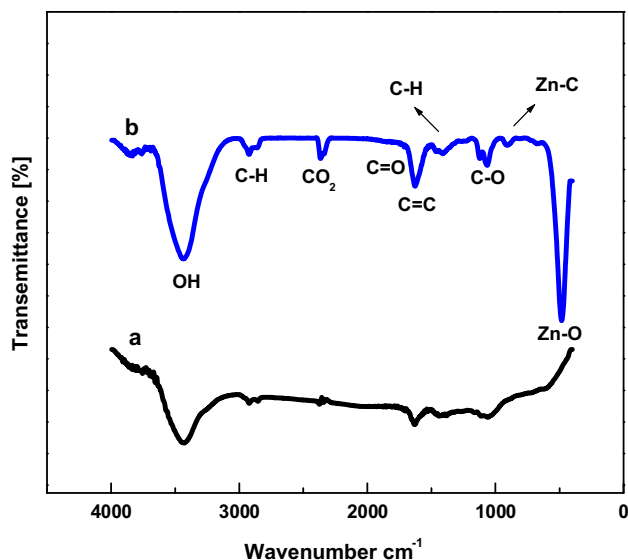


**Fig. 4** FTIR spectra of the **a** MWCNT-COOH and **b** MWCNT-COOH-ZnO [1:3]

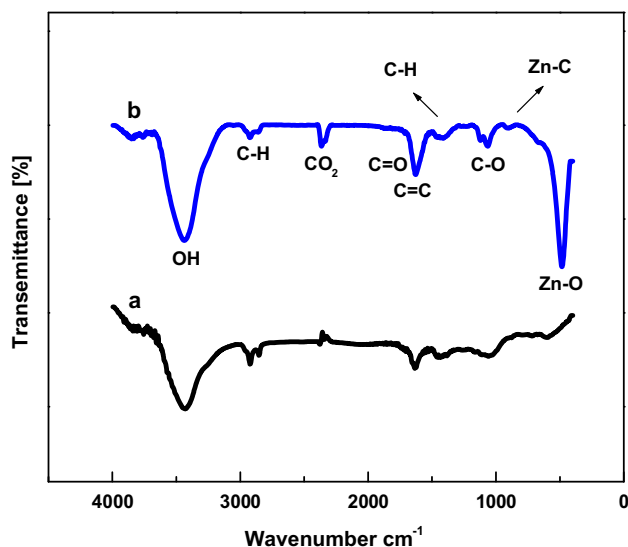
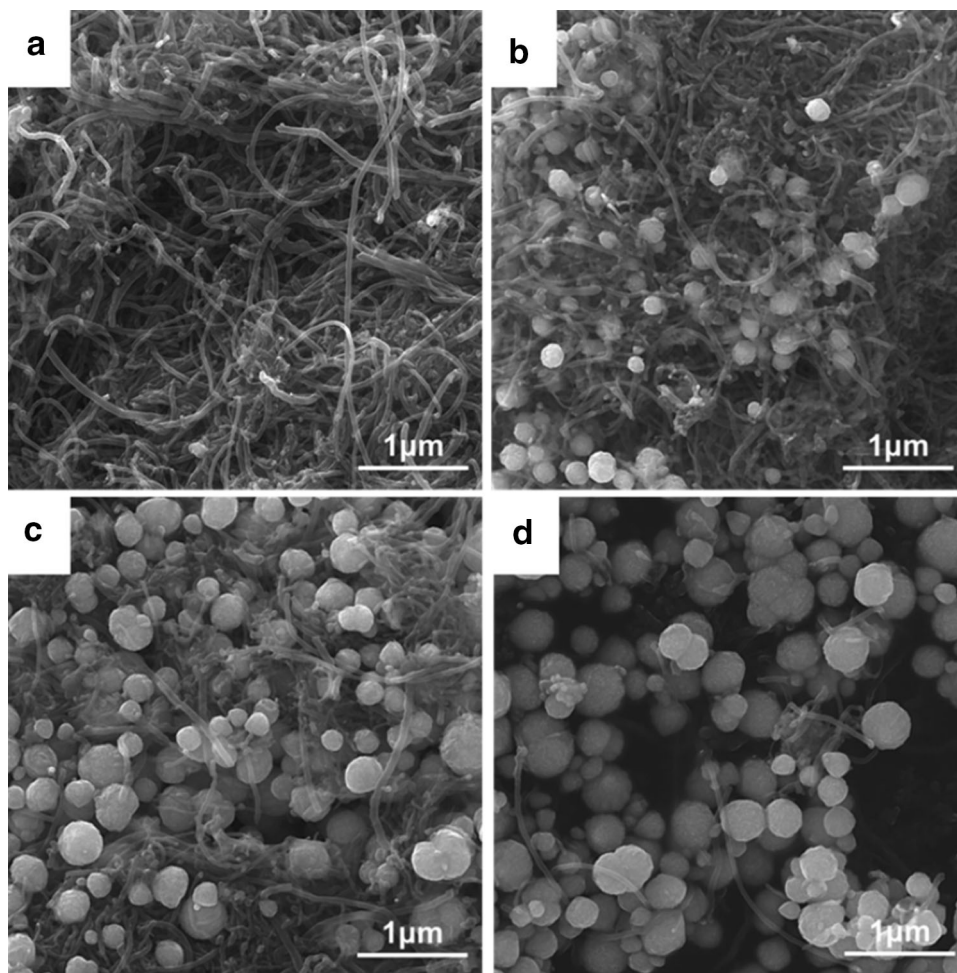


**Fig. 5** FTIR spectra of the **a** MWCNT-OH and **b** MWCNT-OH-ZnO [1:3]

are related to (100), (002) and (101) crystal plates as observed elsewhere [13, 21]. The peak intensities of the CNT and ZnO are different in various samples depended to the concentration ratio of carbon nanotubes and zinc oxide. It can be seen that with increasing the concentration of ZnO precursor, the intensity of the CNTs' peaks (especially at  $26^\circ$ ) dramatically decreases and the peaks of ZnO become stronger. Thus, we can conclude that with increasing the amount of ZnO precursor, more ZnO nanoparticles cover the CNTs' surfaces. Figure 3 represents the XRD patterns of the raw MWCNT-OH and MWCNT-OH-ZnO hybrid

**Fig. 6** FESEM images of the **a** MWCNT-COOH and hybrid samples, **b** MWCNT-COOH-ZnO [3:1], **c** MWCNT-COOH-ZnO [1:1] and **d** MWCNT-COOH-ZnO [1:3]



samples. Similar results were obtained for MWCNT-OH-ZnO hybrid samples.

#### Fourier transform infrared spectroscopy (FTIR)

Fourier transform infrared spectroscopy was performed to understand further the formation of MWCNT-ZnO nanohybrid and the surface chemistry of prepared nanostructures. Figures 4 and 5 show the FTIR spectrum of the raw MWCNT-COOH, MWCNT-OH and typical hybrid samples with concentration ratio of MWCNT-ZnO = 1:3 in the range of 4000–400  $\text{cm}^{-1}$  wave number. In the high frequency region, the absorption peaks at about 3440  $\text{cm}^{-1}$  can be assigned to the bending vibrations of adsorbed molecular water and stretching vibrations of OH groups. The peaks appeared at about 2340  $\text{cm}^{-1}$  correspond to the  $\text{CO}_2$  that adsorbed on the surface of the samples. C-H groups' stretching vibration peaks are at about 2850–2900  $\text{cm}^{-1}$ . The absorption peaks in the range of 1630–1716  $\text{cm}^{-1}$  exhibit the vibration modes of COOH

(C = O and C = C) functional group. In the low frequency or fingerprint region the peaks at about 484 and 910  $\text{cm}^{-1}$  (which are appeared in hybrid samples and are absent in the raw functional CNT spectrums) are related to the Zn-O and Zn-C bonds on the surface of the CNTs. These peaks support the fact that ZnO nanoparticles are synthesized and attached to the surfaces of CNTs [9, 11, 25].

#### Scanning electron microscopy (SEM)

Figure 6 shows the FESEM images of the initial MWCNT-COOH and MWCNT-COOH-ZnO hybrid nanomaterials. Figure 6a shows the filamentous and smooth morphology of initial carboxyl MWCNTs. For hybrid samples (Fig. 6b, c, d) sphere-like nanoparticles on the matrix of CNTs are appeared. Further characterization revealed that these rather spherical particles are ZnO nanoparticles. Thus, the simple sol-gel process resulted in successful growth of CNT-ZnO hybrids. Furthermore, it can be seen that with increasing the concentration ratio of ZnO precursor to



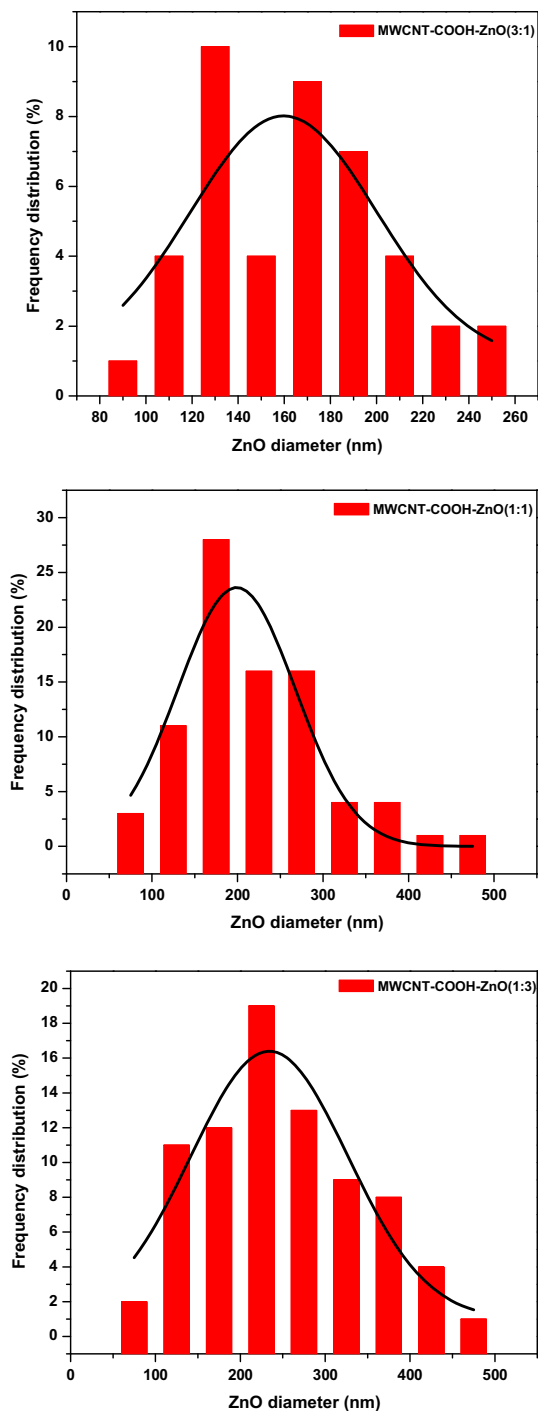


**Fig. 7** Size distribution histograms of ZnO nanoparticles synthesized in MWCNT-COOH-ZnO hybrids

CNT, the number and sizes of attached ZnO nanoparticles on the surface of the MWCNTs are increased. Figure 7 represents the size distribution histograms (derived from SEM images) of ZnO nanoparticles synthesized in MWCNT-COOH-ZnO hybrid nanostructures. Each histogram is fitted by a normal curve. According to these

histograms the average diameter of ZnO nanoparticles in MWCNT-COOH-ZnO hybrid samples with concentration ratio of MWCNT:ZnO = 3:1, 1:1 and 1:3 are 160, 220 and 250 nm, respectively. Figure 8 shows the FESEM images of the initial MWCNT-OH and MWCNT-OH-ZnO hybrid nanomaterials. Similar hybrid morphologies appeared in these samples. Similarly by increasing the concentration of ZnO precursor in nanohybrid preparation, the size and number of ZnO nanoparticles are increased. Histograms of size distribution of ZnO nanoparticles for MWCNT-OH-ZnO nanohybrids are represented in Fig. 9. According to this figure the average diameter of ZnO nanoparticles in MWCNT-OH-ZnO hybrid samples with concentration ratio of MWCNT:ZnO = 3:1, 1:1 and 1:3 are 165, 250 and 260 nm, respectively. Therefore, at the same concentration ratio of ZnO precursor to CNT, relatively smaller ZnO nanoparticles on COOH functionalized CNTs are synthesized compared to OH functionalized ones. Furthermore it seems (compare Fig. 6 with Fig. 8) that the distribution of ZnO nanoparticles in MWCNT-COOH-ZnO hybrids is more uniform and denser compared to MWCNT-OH-ZnO samples.

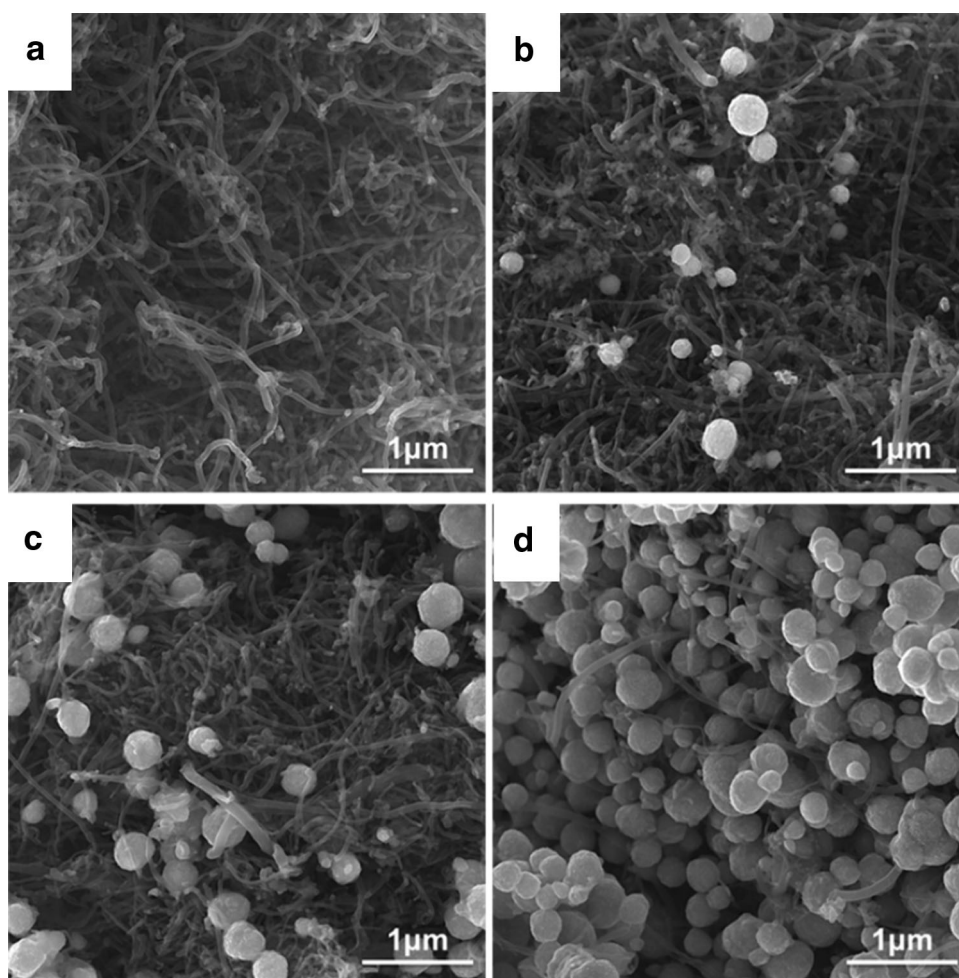
#### Energy dispersive X-ray spectroscopy (EDX)

For further comparison between COOH and OH functionalized CNT-ZnO hybrids, EDX analysis was performed. Figure 10 shows the EDX spectrum of MWCNT-COOH-ZnO hybrid samples. As we expected it confirms the presence of C, O and Zn elements in the hybrid samples. Quantitative results obtained from EDX analysis revealed that the wt% of Zn deposited on the surface of MWCNT-COOH was 12.5, 36.4 and 64.9 for MWCNT:ZnO mass ratio = 3:1, 1:1 and 1:3, respectively. Thus, as we expected the amount of ZnO nanoparticles loaded on the surface of CNTs increases by MWCNT:ZnO ratio as the following trend  $3:1 < 1:1 < 1:3$ . Similar result for MWCNT-OH-ZnO was obtained. The EDX analysis of MWCNT-OH-ZnO revealed that the wt% of Zn deposited on the surface of MWCNT-OH was 10.8, 32.0 and 53.4. The amount of ZnO nanoparticles loaded on the surface of CNTs increases by MWCNT:ZnO ratio as similar trend  $3:1 < 1:1 < 1:3$ . Moreover in comparison between the two functional groups, the amount of ZnO material loaded on the surface of CNTs with COOH functional group is relatively more than that of OH functionalized CNTs.

#### Transmission electron microscopy (TEM)

Figure 11 shows the TEM images of MWCNT-COOH-ZnO hybrid samples. The dark rather spherical morphologies exhibit ZnO nanospheres. As indicated by these

**Fig. 8** FESEM images of the **a** MWCNT-OH and hybrid samples, **b** MWCNT-OH-ZnO [3:1], **c** MWCNT-OH-ZnO [1:1], **d** MWCNT-OH-ZnO [1:3]

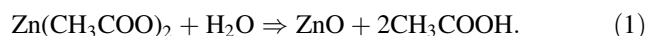


images, the spherical ZnO nanoparticles are attached on the tips or side-walls of CNTs. Unattached separated or isolated ZnO nanospheres were not observed. This observation provides a direct and strong evidence of successful formation of MWCNT-ZnO nanohybrid. By increasing the mass ratio of ZnO precursor to CNTs more and larger ZnO nanoparticles appeared.

In this study the process used to prepare zinc oxide nanoparticles and subsequent hybrid materials is a polyol process [24, 26–29]. The polyol synthesis designates the liquid-phase synthesis in high-boiling, multivalent alcohols and is mainly directed to nanoparticles. Chemically, the polyol family starts with ethylene glycol (EG) as its simplest representative. Based on EG, the polyols comprise two main series of molecules: (1) diethylene glycol (DEG), triethylene glycol (TrEG), tetraethylene glycol (TEG), and so on up to polyethylene glycol (PEG), with the latter containing more than 2000 ethylene groups, (2) propanediol (PDO), butanediol (BD), pentanediol (PD), and so on. Moreover, glycerol (GLY), pentaerythritol (PE), and carbohydrates chemically belong to the polyols [24, 26]. In a typical polyol process, the

solid precursor is suspended in the liquid polyol, and then the solution or the suspension is stirred and heated to a given temperature which can reach the boiling point of the polyol. Polyol is an excellent capping reagent as well as a good dispersive medium, which plays a critical role in the nucleation and growth of the crystalline nanoparticles. For the polyol-mediated synthesis of metal oxides a defined amount of water has to be added into the polyol and the relative concentration of water versus the metal concentration, i.e., the hydrolysis ratio, is a critical parameter to tune the size of the nanoparticles obtained through spontaneous nucleation [26]. The growth mechanism of ZnO coating on the surface of MWCNTs is purposed as follow [27].

The pyrolysis temperature of zinc acetate is about 350 °C, while the maximum reaction temperature of this study is 180 °C. Thus, the formation of ZnO sol is not through pyrolysis but rather hydrolysis process according to the Eq. (1):



After the hydrolysis of zinc acetate, ZnO crystal nuclei are first formed directly, followed by growing up gradually.

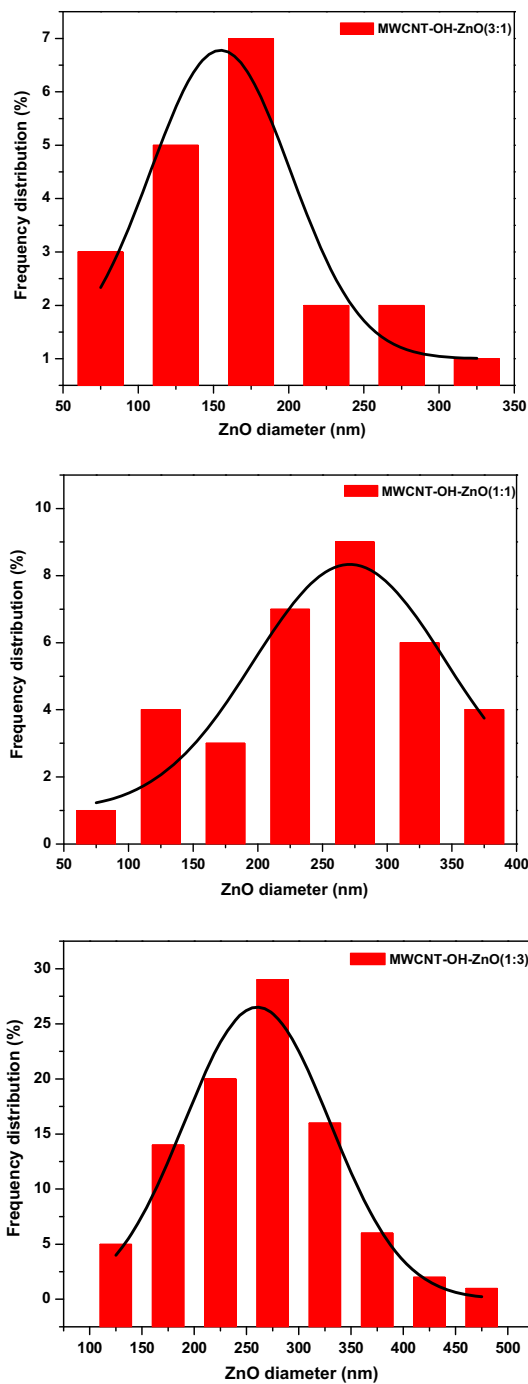


**Fig. 9** Size distribution histograms of ZnO nanoparticles synthesized in MWCNT-OH-ZnO hybrids

Since DEG in the system can react with acetic acid, it speeds up the reaction in Eq. (1). Moreover, the presence of DEG is used as a solvent to raise the viscosity of the solution, which causes the crystallization rate to slow down. Therefore, the system has enough time to form many crystal nuclei and to grow ZnO crystals at high temperatures.

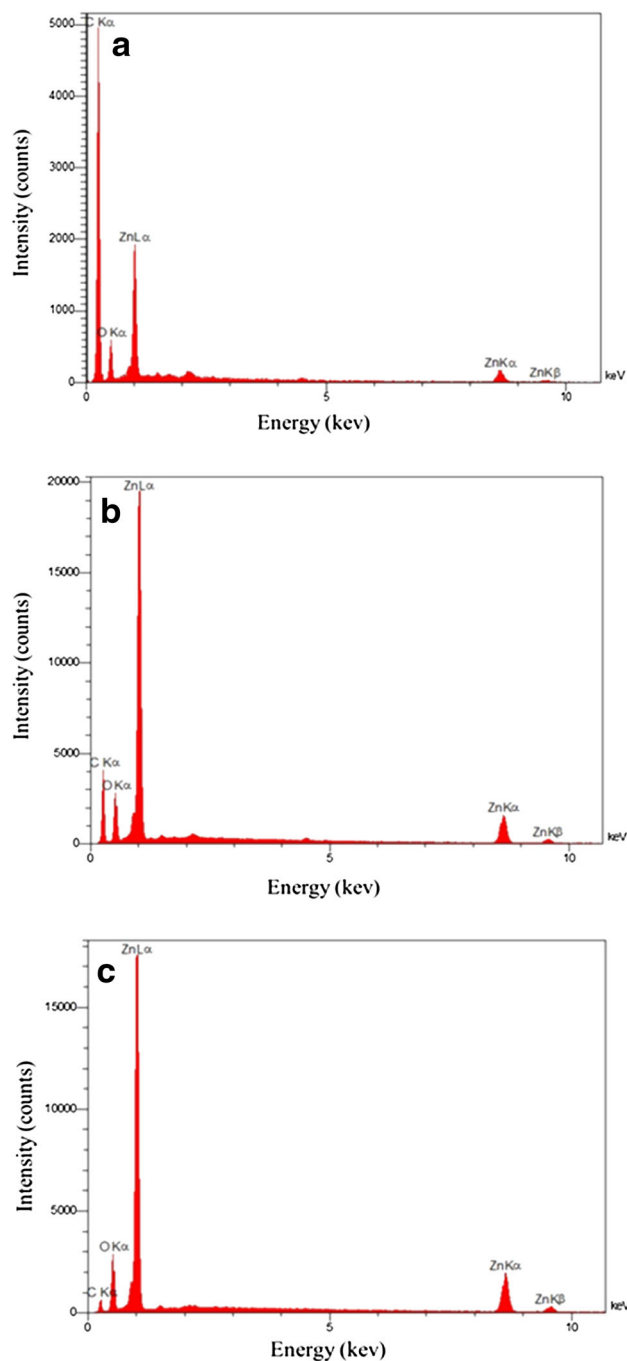
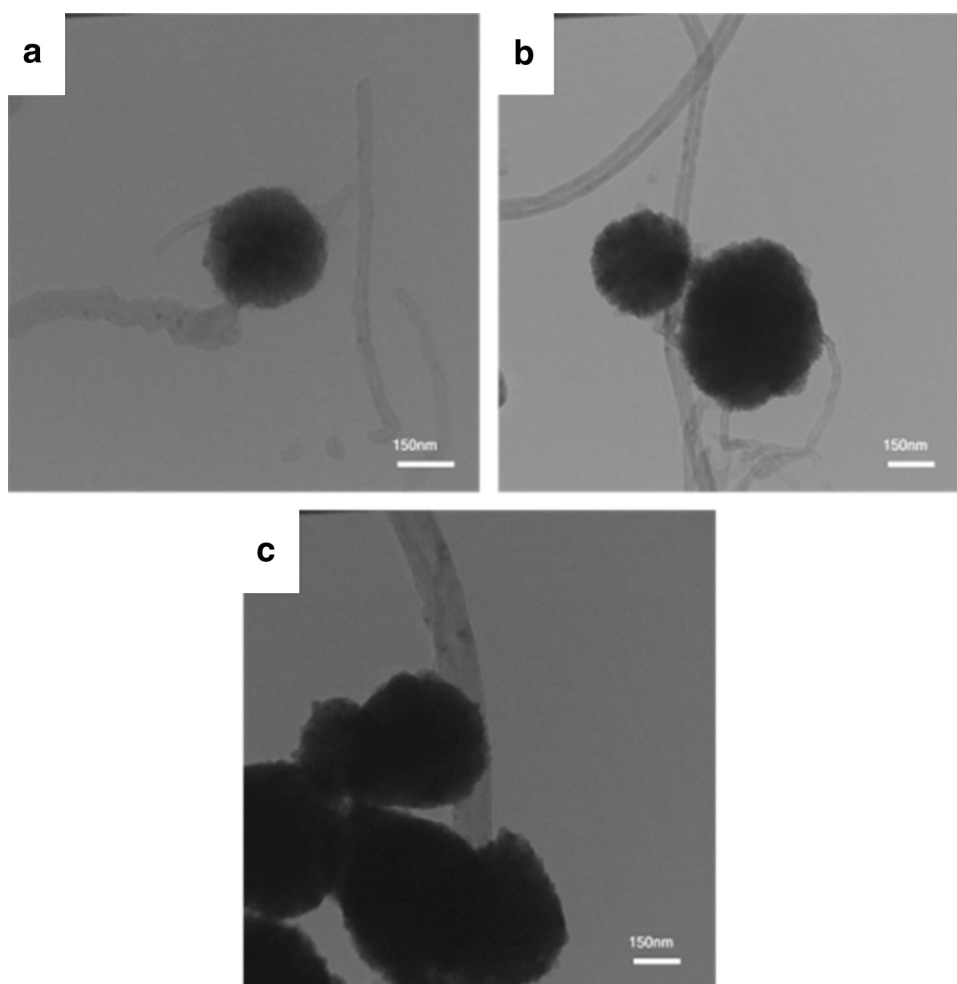


**Fig. 10** EDX analysis of hybrid samples: **a** MWCNT-COOH-ZnO [3:1], **b** MWCNT-COOH-ZnO [1:1] and **c** MWCNT-COOH-ZnO [1:3]

On the other hand, electrical double layers composed of  $Zn^{2+}$  on the surface of ZnO sol particles and acetate anions surrounded these particles [27] provide positive charges and repulsive interactions which stabilize the colloidal sol. Because of the presence of hydroxyl and carboxyl functional groups, the MWCNTs become negatively charged;

**Fig. 11** TEM images of the hybrid samples: **a** MWCNT-COOH-ZnO [3:1], **b** MWCNT-COOH-ZnO [1:1] and **c** MWCNT-COOH-ZnO [1:3]



so the ZnO nanoparticles attach to the MWCNT surfaces by electrostatic attractions [28, 29].

## Conclusions

A simple sol-gel method was used to synthesis the MWCNT-ZnO hybrid nanostructures. Two type of functional MWCNT with COOH and OH functional groups and three concentration ratio of MWCNT:ZnO = 3:1, 1:1 and 1:3 were examined. The appearance of Zn-O and Zn-C vibration modes in FTIR spectrum of hybrid samples revealed the formation of ZnO nanoparticles and attachment of these particles to the surfaces of CNTs. The XRD patterns of hybrid samples support the fact that the ZnO nanoparticles with hexagonal crystal structure decorated the body of CNTs. The SEM observation showed that the ZnO nanoparticles have rather spherical shapes. It was observed that with increasing the concentration of ZnO precursor, the size and number of ZnO nanoparticles which cover the surfaces of CNTs (for both functional groups) were increased. The average diameter of ZnO nanoparticles in MWCNT-

COOH-ZnO (MWCNT-OH-ZnO) hybrid samples with concentration ratio of MWCNT:ZnO = 3:1, 1:1 and 1:3 are 160(165), 220(250) and 250(260) nm, respectively. The average sizes of ZnO nanoparticles decorated the MWCNT-COOH are smaller than that of MWCNT-OH and the amount of ZnO material loaded on the surface of MWCNT-COOH is more than that of MWCNT-OH.

**Open Access** This article is distributed under the terms of the Creative Commons Attribution 4.0 International License (<http://creativecommons.org/licenses/by/4.0/>), which permits unrestricted use, distribution, and reproduction in any medium, provided you give appropriate credit to the original author(s) and the source, provide a link to the Creative Commons license, and indicate if changes were made.

## References

1. De Volder, M.F.L., Tawfick, S.H., Baughman, R.H., Hart, A.J.: Carbon nanotubes: present and future commercial applications. *Science* **339**, 535–539 (2013)
2. Tan, C.W., Tan, K.H., Ong, Y.T., Mohamed, A.R., Zein, S.H.S., Tan, S.H.: Energy and environmental applications of carbon nanotubes. *Environ. Chem. Lett.* **10**, 265–273 (2012)





3. Verma, P., Saini, P., Malik, R.S., Choudhary, V.: Excellent electromagnetic interference shielding and mechanical properties of high loading carbon-nanotubes/polymer composites designed using melt recirculation equipped twin-screw extruder. *Carbon* **89**, 308–317 (2015)
4. Cheng, Y., Xu, C., Jia, L., Gale, J.D., Zhang, L., Liu, C., Shen, P.K., Jiang, S.P.: Pristine carbon nanotubes as non-metal electrocatalysts for oxygen evolution reaction of water splitting. *Appl. Catal. B* **163**, 96–104 (2015)
5. Ghodselahe, T., Solaymani, S., Akbarzadeh Pasha, M., Vesaghi, M.A.: Ni nanoparticle catalyzed growth of MWCNTs on Cu NPs@ aC: H substrate. *Eur. Phys. J. D* **66**, 299–303 (2012)
6. Chen, C.S., Liu, T.G., Lin, L.W., Xie, X.D., Chen, X.H., Liu, Q.C., Liang, B., Yu, W.W., Qiu, C.Y.: Multi-walled carbon nanotube-supported metal-doped ZnO nanoparticles and their photocatalytic property. *J. Nanopart. Res.* **15**, 1295–1304 (2013)
7. Wang, X., Yao, S., Li, X.: Sol-gel preparation of CNT/ZnO nanocomposite and its photocatalytic property. *Chin. J. Chem.* **27**, 1317–1320 (2009)
8. Zhang, W.D., Xu, B., Jiang, L.C.: Functional hybrid materials based on carbon nanotubes and metal oxides. *J. Mater. Chem.* **20**, 6383–6391 (2010)
9. Samadi, M., Shivaee, H.A., Zanetti, M., Pourjavadi, A., Moshfegh, A.: Visible light photocatalytic activity of novel MWCNT-doped ZnO electrospun nanofibers. *J. Mol. Catal. A Chem.* **359**, 42–48 (2012)
10. Yang, M., Liang, T., Peng, Y., Chen, Q.: Synthesis and characterization of a nanocomplex of ZnO nanoparticles attached to carbon nanotubes. *Acta Phys. Chim. Sin.* **23**, 145–151 (2007)
11. Zhu, L.P., Liao, G.H., Huang, W.Y., Ma, L.L., Yang, Y., Yu, Y., Fu, S.Y.: Preparation, characterization and photocatalytic properties of ZnO-coated multi-walled carbon nanotubes. *Mater. Sci. Eng. B* **163**, 194–198 (2009)
12. Wang, X., Xia, B., Zhu, X., Chen, J., Qiu, S., Li, J.: Controlled modification of multiwalled carbon nanotubes with ZnO nanostructures. *J. Solid State Chem.* **181**, 822–827 (2008)
13. Chen, C.S., Chen, X.H., Yi, B., Liu, T.G., Li, W.H., Xu, L.S., Yang, Z., Zhang, H., Wang, Y.G.: Zinc oxide nanoparticle decorated multi-walled carbon nanotubes and their optical properties. *Acta Mater.* **54**, 5401–5407 (2006)
14. Dalouji, V., Elahi, S.M., Solaymani, S., Ghaderi, A.: Absorption edge and the refractive index dispersion of carbon-nickel composite films at different annealing temperatures. *Eur. Phys. J. Plus* **131**, 1–6 (2016)
15. Eder, D.: Carbon nanotube–inorganic hybrids. *Chem. Rev.* **110**, 1348–1385 (2010)
16. Kołodziejczak-Radzimska, A., Markiewicz, E., Jesionowski, T.: Structural characterization of ZnO particles obtained by the emulsion precipitation method. *J. Nanomater.* **15**, 1–9 (2012)
17. Ramar, A., Soundappan, T., Chen, S.M., Rajkumar, M., Ramiah, S.: Incorporation of multi-walled carbon nanotubes in ZnO for dye sensitized solar cells. *Int. J. Electrochem. Sci.* **7**, 11734–11744 (2012)
18. Lv, T., Pan, L., Liu, X., Sun, Z.: Enhanced photocatalytic degradation of methylene blue by ZnO-reduced graphene oxide–carbon nanotube composites synthesized via microwave-assisted reaction. *Catal. Sci. Technol.* **2**, 2297–2301 (2012)
19. Tãlu, Ș., Bramowicz, M., Kulesza, S., Solaymani, S., Ghaderi, A., Dejam, L., Elahi, S.M., Boochani, A.: Microstructure and micromorphology of ZnO thin films: case study on Al doping and annealing effects. *Superlattices Microstruct.* **93**, 109–121 (2016)
20. Akhavan, O., Azimirad, R., Safa, S.: Functionalized carbon nanotubes in ZnO thin films for photoinactivation of bacteria. *Mater. Chem. Phys.* **130**, 598–602 (2011)
21. Jiang, L., Gao, L.: Fabrication and characterization of ZnO-coated multi-walled carbon nanotubes with enhanced photocatalytic activity. *Mater. Chem. Phys.* **91**, 313–316 (2005)
22. Tang, Z.K., Wong, G.K., Yu, P., Kawasaki, M., Ohtomo, A., Koinuma, H., Segawa, Y.: Room-temperature ultraviolet laser emission from self-assembled ZnO microcrystallite thin films. *Appl. Phys. Lett.* **72**, 3270–3272 (1998)
23. Ahmad, M., Ahmed, E., Hong, Z.L., Ahmed, W., Elhissi, A., Khalid, N.R.: Photocatalytic, sonocatalytic and sonophotocatalytic degradation of Rhodamine B using ZnO/CNTs composites photocatalysts. *Ultrason. Sonochem.* **21**, 761–773 (2014)
24. Dong, H., Chen, Y.C., Feldman, C.: Polyol synthesis of nanoparticles: status and options regarding metals, oxides, chalcogenides, and non-metal elements. *Green Chem.* **17**, 4107–4132 (2015)
25. Saleh, T.A., Gondal, M.A., Drmosh, Q.A., Yamani, Z.H., Al-Yamani, A.: Enhancement in photocatalytic activity for acetaldehyde removal by embedding ZnO nano particles on multiwall carbon nanotubes. *Chem. Eng. J.* **166**, 407–412 (2011)
26. Fievet, F., Brayner, R.: The polyol process. In: Brayner, R., Fievet, F., Coradin, T. (eds.) *Nanomaterials: a danger or a promise?*, pp. 1–25. Springer, London (2013)
27. Yu, Y., Huang, W.Y., Li, J.L., Ma, L.L.: Preparation and photocatalytic property of ZnO/MWCNTs composites. In: Buckley, R.W. (ed.) *Solid state chemistry research trends*, pp. 1–22. Nova Science Publishers, Inc., New York (2007)
28. Yu, Y., Ma, L.L., Huang, W.Y., Li, J.L., Wong, P.K., Yu, J.C.: Coating MWNTs with Cu<sub>2</sub>O of different morphology by a polyol process. *J. Solid State Chem.* **178**, 1488–1494 (2005)
29. Jia, B., Gao, L., Sun, J.: Self-assembly of magnetite beads along multiwalled carbon nanotubes via a simple hydrothermal process. *Carbon* **45**, 1476–1481 (2007)

